PCCP

ROYAL SOCIETY OF CHEMISTRY

PAPER

View Article Online
View Journal

Cite this: DOI: 10.1039/d0cp03612a

Theoretical study on the absorption of carbon dioxide by DBU-based ionic liquids†

Mohammad Izadyar, *[a] Mojtaba Rezaeian[a] and Alexey Victorov[b]

Received 6th July 2020,
Accepted 15th August 2020

DOI: 10.1039/d0cp03612a

rsc.li/pccp

In this article, 20 ns molecular dynamic (MD) simulations and density functional theory (DFT) were used to investigate the absorption of CO_2 molecules by some functionalized 1,8-diazabicyclo[5,4,0]-udec-7-ene (DBU)-based ILs. According to the MD results, the highest coordination number for N···C is observed in the case of **[DBUH$^+$][Im$^-$]**, which indicates that the functionalization of the imidazole anion by different alkyl groups decreases the interaction ability of the anion with CO_2 molecules. The addition of water molecules to the ILs decreases the ability of the anion to interact with CO_2 because of the hydrogen bond formation between the imidazole anions and water. Two different paths were proposed for CO_2 absorption by the ILs, and the effect of alkyl groups on the kinetics and thermodynamics of the reaction was analyzed by using the M06-2X functional at the 6-311++G(d,p) level of theory in the gas phase and water. On the basis of the results, CO_2 absorption is more favorable in **[DBUH$^+$][Im$^-$]**, thermodynamically. Kinetic parameters show that the alkylation of the imidazole anion by ethyl, propyl, iso-propyl, and phenyl groups decreases the rate of CO_2 absorption, because of the steric and electron-withdrawing effect of different alkyl groups. In the presence of water molecules, the lowest activation Gibbs energy is related to **[DBUH$^+$][Im$^-$]**, which confirms the greater ability of this IL in CO_2 absorption.

1. Introduction

In recent years, the atmosphere has been changed by greenhouse effects. Carbon dioxide (CO_2) was found to be able to effectively increase the earth's temperature and produce the global warming problem.[1–3] Moreover, gaseous compounds such as shale gas, natural gas, and biogas have CO_2 impurities, which affects the cost of thermal energy sources.[4] In the last decade, the CO_2 concentration in the atmosphere has increased due to industrial activities.[5] Therefore, the purification of gases is a significant topic investigated by different research groups.[6] Amine solutions are efficient absorbents for CO_2 separation, but these solvents have some limitations in industrial applications, such as toxicity, corrosiveness, and destructive environmental effects.[7,8]

Ionic Liquids (ILs) have a melting point below 100 °C containing organic cations and organic or inorganic anions,[9,10] as well as outstanding properties, such as non-flammability, non-volatility, no toxicity, and biodegradability.[11,12] These properties make them favorable for different applications in catalysis,[13] biochemistry, enzymes,[14] chemical industries,[15] and green chemistry.[16] In comparison with the amine solution, ILs have emerged as a potential candidate for use as an absorbent in CO_2 capture.[17] For instance, in amino acid ILs, the presence of the amine and carboxylate group in the anion structure provides a good capacity for CO_2 absorption.[18] The structure tunability of the ILs is more than that of an amine solution, which makes them favorable for designing diversity in the cation and anion parts for efficient CO_2 capture.[19]

A new generation of compounds based on 1-8-diazabicyclo [5,4,0]-udec-7-ene (DBU) was discovered by Moller's group.[20] For the first time, DBU-based compounds were used as the catalysts by Bertrand's group, because of their ability of nucleophilic attack in organic reactions.[21] DBU-based compounds have been used in the organic synthesis of switchable ionic liquids (SILs) as a new generation of solvents that have numerous applications in extraction,[22] biochemistry,[23] CO_2 absorption,[24] and catalysis[25] because of their non-nucleophilic alkaline nature.

Privalova *et al.* studied DBU-based ILs having the alcohol group as the SILs (ROH, R = 1-hexanol, 6-amino-1-hexanol) for CO_2 absorption.[26] The results show that in comparison with the classical ILs, SILs have a high CO_2 absorption capacity. The viscosity of the SILs is higher than that of classical ILs that decreases with temperature increment. On the basis of the obtained results, they suggested that these types of ILs can be applied for CO_2 absorption in industry.

Lethesh and coworkers studied the density, viscosity, surface tension, and thermal stability of twelve kinds of DBU-based ILs

[a] Computational Chemistry Research Laboratory, Department of Chemistry, Faculty of Science, Ferdowsi University of Mashhad, Mashhad, Iran. E-mail: izadyar@um.ac.ir; Fax: +98 5138805533
[b] Department of Chemistry, St. Petersburg State University, Universitetskaya nab. 7/9, St. Petersburg 199034, Russia

† Electronic supplementary information (ESI) available. See DOI: 10.1039/d0cp03612a

with chloride, bromide, and thiocyanate anions.[27] The obtained results confirm that an increase in the length of the alkyl groups in the DBU cation increases the viscosity of the ILs. The surface tension of these ILs is more than that of common solvents and lower than that of imidazolium-based ILs. Based on the experiments, they claimed that the thermal stability of the DBU-based ILs is approximately equal to the imidazolium type.

Chen and coworkers synthesized 3(2*H*)furanones from diyne alcohols in the presence of DBUH-based ILs as the catalyst.[28] They found that the basic ability of the imidazole anion has a significant effect on the catalytic activity of the ILs. NMR data and density functional theory (DFT) results indicate that the imidazole anion functionalized by benzyl groups has the highest basicity and catalytic activity in comparison with other ILs. They inferred that the benzyl group improves the performance of the DBU-based ILs as the solvent in chemical reactions.

In particular, the IL solvents have some water impurities and the presence of water molecules has an important effect on the properties of ILs.[29] The results indicated that the formation of a strong hydrogen bond between the water and ILs affects the reactivity of them.

Zhu and coworkers investigated a new generation of protic ILs with DBU as the cation and imidazole as the anion.[30] The results show that CO_2 absorption proceeds in a stoichiometric ratio of 1 : 1. The effects of water and anion functionalization were investigated and the obtained results demonstrate that the functionalization of the anion by different substitution groups plays an important role in CO_2 absorption and the rate of CO_2 uptake decreases in the presence of water. They examined the recyclability and reusability of **[DBUH$^+$][Im$^-$]** IL by absorption/desorption diagrams. The obtained results indicate that **[DBUH$^+$][Im$^-$]** IL maintains the ability of CO_2 absorption during the recycling process with a slight weight loss, which makes them suitable for industrial application.

The recyclability and reusability of the [DBU][Lac] ILs were investigated in the reaction between aniline and 2-cyclohexen-1-one.[31] The obtained results indicate that this IL can be reused in 8 cycles without any decrease in the catalytic activity. In another study, the reaction between propargylic amine and CO_2 was catalyzed by [DBUH][MIm] IL.[32] The obtained results confirm that this IL can be reused for five cycles without mass and catalytic activity loss, which makes it favorable for industrial applications.

Li *et al.* studied the cycloaddition of CO_2 with the epoxide ring in the presence of DBU-based ILs.[33] Different kinds of cations were used including DBU, 1,5-diazabicyclo[4,3,0]-5-nonene (DBN), and imidazolium. The results showed that DBU-based ILs have better catalytic activity than other ones. The effects of temperature, pressure, and time of reaction were investigated to specify the optimum conditions for the reaction. The obtained results show that the best conditions are 120 K, 1 MPa, and 2.5 h. DFT calculations were performed to investigate the hydrogen bond interaction between the ILs and the reactant for proposing the best mechanism of this reaction.[33] On the basis of the energy analysis, the absorption of CO_2 by the epoxide ring in the presence of the ILs as the catalyst is the preferred mechanism.

Wang *et al.* investigated the effect of DBU super base and DBU-derived bromide ILs in the reaction between CO_2, amine, and epoxide.[34] NMR spectroscopy and DFT calculations were performed to investigate the mechanism of the reaction. The results showed that DBU-based ILs and DBU super base act as the hydrogen donors and acceptors, respectively. In other words, DBU and DBU-based ILs are found as cooperative activators for the substrate. Therefore, a mixture of organic solvents, such as DBU super base and DBU-based ILs can be identified as a synergetic catalyst for the mentioned reaction.

DFT calculations and molecular dynamic (MD) simulations are powerful methods to examine the interaction of the IL–CO_2 from the molecular viewpoint. Zhang *et al.* reported that guanidinium-based ILs can be used for CO_2 absorption.[35] MD simulations and DFT calculations were employed to investigate the CO_2 absorption at different concentrations. The radial distribution function (RDF) and coordination number ($N(r)$) show the closer affinity of [BF_4^-] anions to CO_2 molecules in comparison with the cation, which indicates that the role of the anion is more important than that of the cation for interaction with CO_2. Also, the DFT results show that the interaction of the anion and CH_3 group of the cation is related to hydrogen bond formation.

As discussed above, DBUH$^+$-based ILs as the cation and imidazole as the anion have suitable physicochemical properties that make them appropriate for use in industrial processes. Also, the imidazole anion is a good candidate for CO_2 absorption because of the high basicity and the presence of two nitrogen atoms in the chemical structure that provide a high ability for interaction with CO_2. Meanwhile, the activity of the DBU-based IL does not change during the absorption process, which makes them suitable for recycling and reusing in industrial processes.

The presence of water molecules has an important effect on the interaction of ILs with CO_2 molecules. Also, it is indicated that the charge distribution in the imidazole ring can affect the interaction ability of CO_2 with imidazole anions. Therefore, the investigation on the effect of substitution groups and the presence of water molecules is important, especially from the molecular viewpoint that provides important data for industrial applications.

Herein, MD simulations and DFT calculations are performed on the eight types of DBU-based ILs consisting of DBU$^+$ as the cation and eight functionalized imidazoles as the anions to examine the ability of these ILs for CO_2 absorption. This study is of interest from the molecular engineering viewpoint for designing new ILs having tunable properties. The structures of the studied DBU-based ILs are shown in Scheme 1.

2. Theoretical methods

2.1. Molecular dynamics simulations

Molecular dynamic simulations were performed to investigate the defined systems including ILs, CO_2, and water molecules by using AMBER 12.[36] The atomic charges of different atoms were

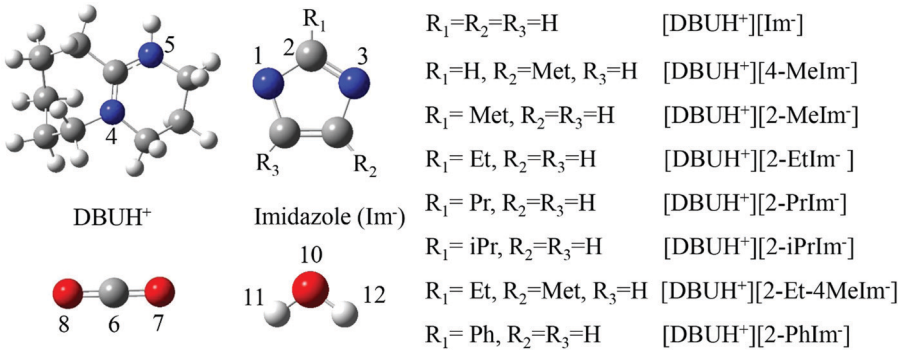

Scheme 1 The structures of DBU-based ILs with eight imidazole groups (Met = methyl, Et = ethyl, Pr = propyl, iPr= iso-propyl, Ph = phenyl), CO_2, and water molecules.

calculated by using the CHelpG method for cations and anions of the ILs, CO_2, and H_2O molecules at the M06-2X/6-311++G(d,p) level of theory.[37] The General Amber Force Field (GAFF) was used to construct the force field parameters by using the antechamber program.[38] To investigate the type and strength of the interactions between the DBU-based ILs and CO_2 molecules, a cubic box with 40 Å dimensions was designed by using the PACKMOL program, which is composed of 150 ion pairs of the ILs and 150 CO_2 molecules.[39]

In the first step of the simulation, energy minimization was applied in 20 000 steps to obtain the optimized structure in terms of energy and reduces unfavorable contacts. After this step, all structures in the *NVT* ensemble were heated from 0 to 300.0 K and 400 ps (according to experimental data). The equilibration step was performed without any positional restraints for 1 ns in the *NPT* ensemble in a pressure of 1 bar and a temperature of 300.0 K. Finally, the results of the equilibration step were used for 20 ns simulations in an *NPT* ensemble (the product stage) with 2 fs time step.

To investigate the effect of water, 150 water molecules were added explicitly in a cubic box of DBU-based ILs. Minimization, heating, equilibration, and production steps were performed under the same conditions for various DBU-based ILs, in the presence of water. The temperature and pressure in the *NPT* ensemble were controlled by using the Langevin thermostat with a collision frequency of 2 ps^{-1} and a relaxation time of 1 ps, respectively.[40,41] The SHAKE constraints were applied including hydrogen bonds with 2 fs time step.[42] The long-range electrostatic interactions were applied by using the Particle Mesh Ewald (PME) method and dispersion interaction was evaluated in a space cut-off of 8 Å.[43]

2.2. DFT calculations

The DFT method was applied to investigate the CO_2 absorption by DBU-based ILs by using the Guassian09 program.[44] The M06-2X functional with the 6-311++G(d,p) basis set was used to optimize the reactants, products, and transition state (TS) structures.[45,46] The zero-point vibrational energy (ZPVEs) was considered for the stationary states. The vibrational frequency analysis confirmed the reactant and product structures with the real frequencies and TS structures with one imaginary frequency. The synchronous transit-guided quasi-Newton (STQN) was employed to locate the TS structure and intrinsic reaction coordinate calculations were used to confirm the stationary point connection.[47]

Water molecules as the solvent affect the thermodynamics and kinetics of CO_2 absorption. Therefore, the solvent effects were investigated by the conductor-like polarizable continuum model (CPCM).[48,49]

Natural bond orbital (NBO) analysis was applied to evaluate the charge transfer between the anion of the DBU-based-ILs and CO_2 in the reactants, products, and TS structure. This analysis was suggested by Reed *et al.* for evaluating donor–acceptor interactions through the second-order perturbation energies, $E(2)$, especially in the TS structure.[50]

To examine the bond critical points (BCPs) of the reactant, product, and TS structures, topological properties were calculated by Bader's quantum theory of atoms in molecules (QTAIM).[51] These parameters include the electron density ($\rho(r)$), kinetic energy density ($K(r)$), potential energy density ($V(r)$), electron location function (ELF), and localized orbital locator (LOL) that were calculated by Multiwfn 3.1.[52]

3. Results and discussion

3.1. MD simulation results

3.1.1 The interaction of CO_2 with imidazole anions. The interaction of the anion–CO_2 during 20 ns simulations was analyzed. The experimental and theoretical results indicate that the anion has an important role in CO_2 absorption.[30] The radial distribution function (RDF) diagrams describe the probability of finding, $g(r)$, and the separated distance, r_{max}, between two atoms that are used to understand the ability of interaction at the special site.[35] In the interaction between the anion, cation, and CO_2 molecules, the lower r_{max} represents the closer affinity of the anion or cation to CO_2 and their stronger interaction.[35] The RDF diagrams for N1···C6 and N3···C6 interactions in the anion–CO_2 are shown in Fig. 1. Also, the RDF diagram for N4···C6 interaction between the cation–CO_2, during 20 ns MD simulations, is shown in Fig. S1 (ESI†). According to the obtained results, the r_{max} value between N1···C6 and N3···C6 is 3.35 Å in different imidazole anions, which is shorter than

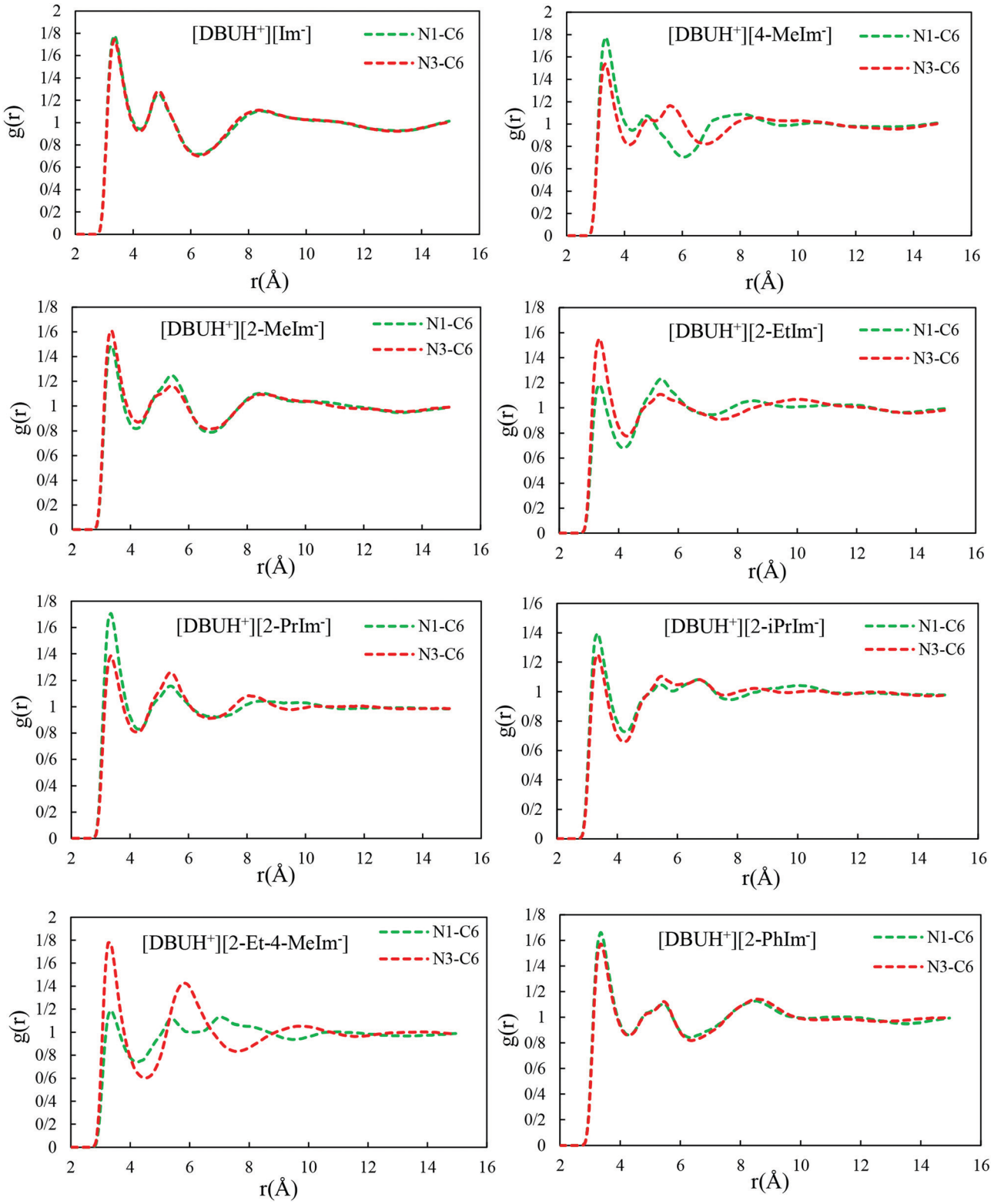

Fig. 1 The calculated RDF for the interaction of N1···C6 and N3···C6 between the anion and CO_2 after 20 ns MD simulations (for atom numbering see Scheme 1).

that of N4···C6 interaction (in the range of 5.55 to 6.25 Å) confirming the effective interaction between CO_2 and imidazole anions.

The first coordination number, $N(r)$, is the area under the first RDF peak used to examine the average number of specific atoms around the central sites. This parameter is useful for

comparison between the strength of the interactions, especially in the cases having equal r_{max}. The coordination number diagram is depicted in Fig. 2. Also, the $g(r)_{max}$ and $N(r)$ values of the N1···C6 and N3···C6 interactions are represented in Table 1.

It was claimed by Zhang *et al.* that the strength of the interaction between CO_2 and the imidazole anion is improved by increasing the $N(r)$ value.[35] According to Table 1, in the case of **[DBUH$^+$][Im$^-$]**, the highest values of $N(r)$ for the N1···C6 and

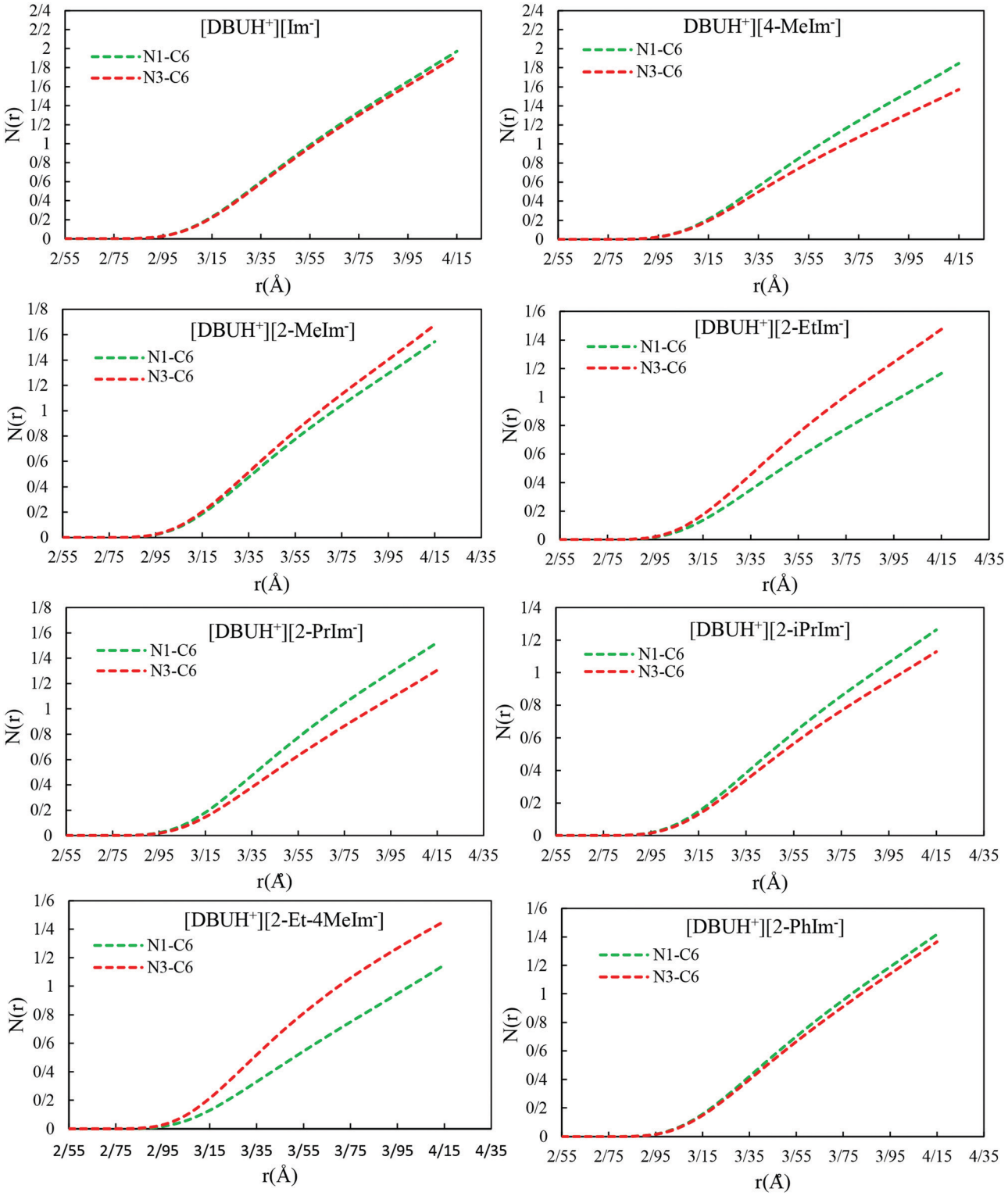

Fig. 2 The coordination number ($N(r)$) for the interaction of N1···C6 and N3···C6 between the anion and CO_2 after 20 ns MD simulations (for atom numbering see Scheme 1).

Table 1 The theoretical value of $g(r)_{max}$ and $N(r)_{max}$ in different DBU-based ILs for N1···C6 and N3···C6 interactions

Compound	$g(r)_{max}$ N1···C6	$N(r)$ N1···C6	$g(r)_{max}$ N3···C6	$N(r)$ N3···C6
[DBUH$^+$][Im$^-$]	1.78	2.14	1.74	2.08
[DBUH$^+$][4-MeIm$^-$]	1.78	2.00	1.52	1.57
[DBUH$^+$][2-MeIm$^-$]	1.48	1.55	1.61	1.68
[DBUH$^+$][2-EtIm$^-$]	1.18	1.17	1.55	1.59
[DBUH$^+$][2-PrIm$^-$]	1.71	1.64	1.38	1.42
[DBUH$^+$][2-iPrIm$^-$]	1.39	1.37	1.25	1.22
[DBUH$^+$][2-Et-4-MeIm$^-$]	1.18	1.25	1.76	1.73
[DBUH$^+$][2-PhIm$^-$]	1.66	1.53	1.57	1.48

N3···C6 interactions are 2.14 and 2.08, respectively, which indicates the strongest interaction between CO_2 and the unsubstituted imidazole anion. In the case of other ILs, the $N(r)$ value for N1···C6 and N3···C6 interaction decreases in the presence of methyl, ethyl, propyl, iso-propyl, and phenyl groups in comparison with **[DBUH$^+$][Im$^-$]**. These results show that the strength of the interactions between CO_2 and the imidazole anion decreases by the substitution of the anion by different alkyl groups.

The $N(r)$ value for the N1···C6 interaction in the case of **[DBUH$^+$][2-MeIm$^-$]** is lower than **[DBUH$^+$][4-MeIm$^-$]**, which indicates that the substitution at the R_1 position by alkyl groups decreases the strength of the interaction greater than that of R_2. Also, multi-substitution in the case of **[DBUH$^+$][2-Et-4-MeIm$^-$]** decreases the strength of interaction in comparison with **[DBUH$^+$][Im$^-$]**. **[DBUH$^+$][2-PhIm$^-$]** has a lower $N(r)$ than **[DBUH$^+$][Im$^-$]**. This result demonstrates that the electron-withdrawing groups decrease the charge density of N1 and N3 atoms of the imidazole anion, which reduces the interaction ability of these atoms with CO_2 molecules.

Overall, the obtained results indicate that the steric hindrance of the alkyl groups and electron-withdrawing effects of the phenyl groups are important factors that decrease the ability of CO_2 interaction with the anion in comparison with **[DBUH$^+$][Im$^-$]**. These results are in agreement with the experimental data, which demonstrate that **[DBUH$^+$][Im$^-$]** has the highest capacity of CO_2 uptake that decreases by the alkyl substitution of the anion.[30]

3.1.2 The effect of water on the anion–CO_2 interaction. On the basis of the experimental data,[30] the CO_2 absorption capacity of the DBU-based ILs significantly decreases in the presence of water. Therefore, to examine the effect of water on the interactions between the imidazole anion and CO_2, 20 ns MD simulations were performed in the presence of 150 water molecules. The RDF diagrams for the interactions of N1 and N3 atoms of the imidazole with the C6 atom of CO_2 are depicted in Fig. S2 (ESI†). The coordination number in the presence of water molecules, $N(r)$, for anion–CO_2 interactions was calculated and shown in Fig. S3 (ESI†). Also, theoretical values of r_{max}, $N(r)$, and $g(r)_{max}$ are represented for the N1···C6 and N3···C6 interactions in Table S1 (ESI†).

According to Table S1 (ESI†), $g(r)_{max}$ and $N(r)$ values of the N1···C6 and N3···C6 interactions in the presence of water are lower than that of pure ILs, implying that the ability of interactions between the anion–CO_2 decreases in the presence of water molecules, in agreement with the experimental data.[29] On the basis of the results, the maximum value of $N(r)$ is related to **[DBUH$^+$][Im$^-$]** and the alkyl substitution on the imidazole anion reduces $N(r)$. According to this result, the substitution of alkyl groups at the R_1 and R_2 positions decreases the ability of interaction between the anion–CO_2 in comparison with **[DBUH$^+$][Im$^-$]**.

To have a better insight into the effect of water, the RDFs for interactions between the O and H atoms of water molecules with N1 and N3 atoms of the imidazole anions were analyzed and represented in Fig. 3. The $g(r)_{max}$ and r_{max} values are represented in Table S2 (ESI†). According to Fig. 3, the strong interactions are related to N1···H11, N3···H11, and O10···H9 pairs.

Three kinds of hydrogen bonds were proposed by Steiner and Jeffry including the strong H-bond (covalent) with the bond distance of 1.2–1.5 Å, moderate H-bond with the bond distance of 1.5–2.2 Å, and weak H-bond with the bond length greater than 2.2 Å.[53] In the case of N1–H11 and N3–H11 interactions, the first sharp peak at 1.85 Å confirms the moderate hydrogen bond formation with electrostatic nature. On the basis of the results, the presence of the water molecule decreases the capacity of CO_2 absorption of DBU-based ILs because of the moderate hydrogen bond formation between the anion and water molecules. According to the Steiner and Jeffry data, the strong, moderate, and weak H-bond angle are greater than 170°, 130° and 90°, respectively. The average H-bond angles are listed in Table S3 (ESI†). These results show that the average H-bond angles between the imidazole anion and water molecules are in the range of 160–162° in different DBU-based ILs, confirming the moderate H-bond formation in the presence of water molecules.

The experimental results indicate that water remarkably affects the rate of CO_2 absorption by the **[DBUH$^+$][Im$^-$]** IL, which is confirmed by the hydrogen bond formation between water molecules and imidazole anions through the MD simulations. This type of H-bond formation may be the main factor that decreases the ability of anions to interact with CO_2 molecules.

3.2. DFT results

3.2.1 Mechanism insight. The interaction between the nitrogen atoms of the DBUH$^+$ and CO_2 was inhibited thermodynamically because of a positive charge of DBUH$^+$ and super basicity of DBU. But two nitrogen atoms of the imidazole anion have a high possibility of interaction with CO_2 because of their negative electronic charge, which is stabilized by the resonance effect.[54,55] The carbamate formation was confirmed by IR spectroscopic and ^{13}C-NMR analyses showing the N–C bond formation (two peaks at 1700 cm^{-1} and 163.5 ppm, respectively). Therefore, we proposed a stoichiometric ratio of 1 : 1 for the absorption mechanism by the DBU-based ILs (Scheme 2), in which carbamate is the main product confirmed by Zhou, experimentally.[30]

3.2.2 Structural analysis. In the mechanism study, we anticipate the strong interaction between the C atom of CO_2 and N atoms of the imidazole anion. This process is conducted

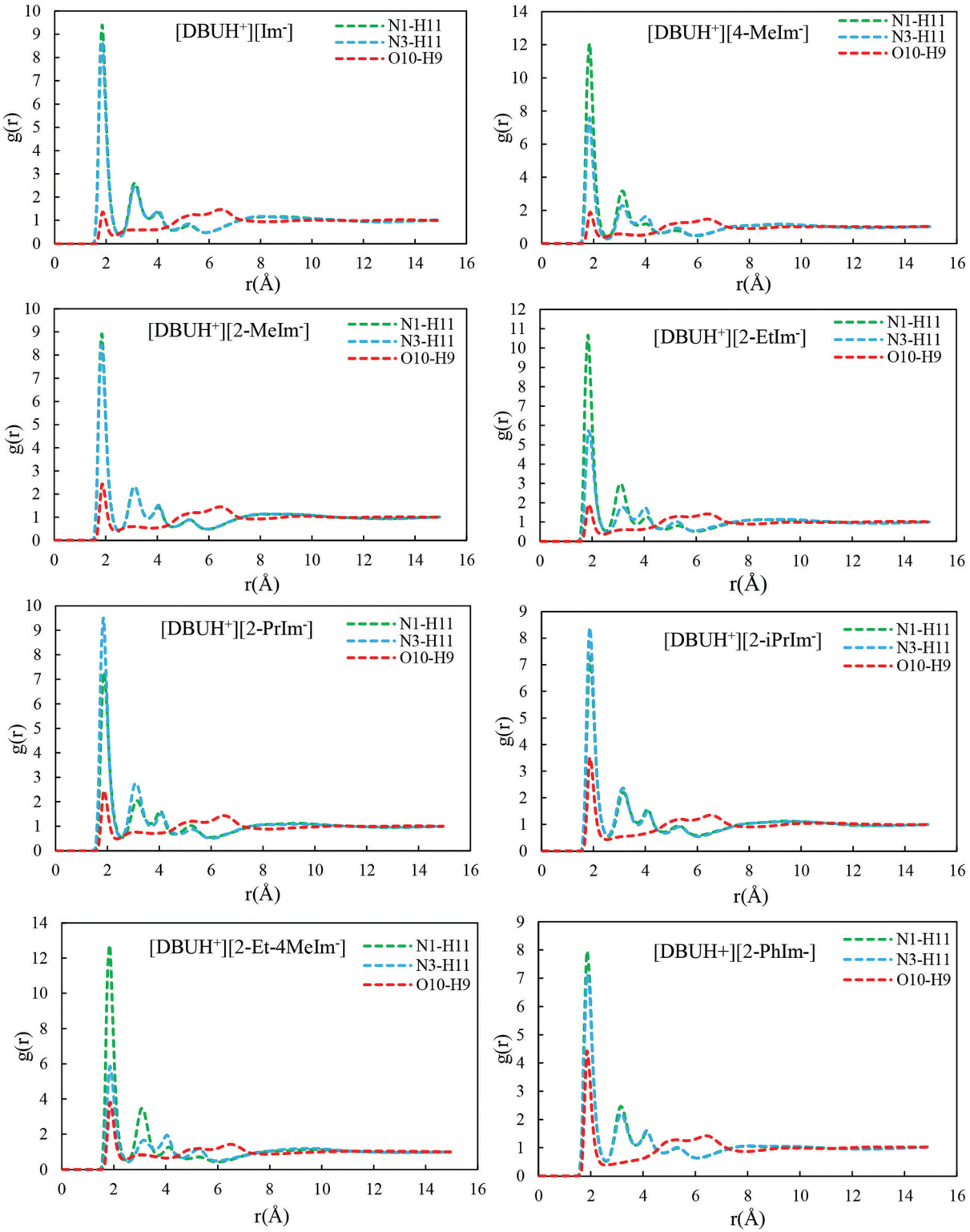

Fig. 3 The calculated RDF for interaction between the functionalized imidazole anion and water molecules after 20 ns MD simulation between O10···H9, N3···H11, and N1···H11 atoms in the presence of water molecules.

by the nucleophile attack of the lone pair electrons of N1 and N3 atoms to the C atom of CO_2. The optimized structure of the reactants, TSs, and product in **[DBUH$^+$][Im$^-$]** IL in the proposed paths are shown in Fig. 4 including the atom numbering.

According to the bond length changes during the CO_2 absorption, Table S4 (ESI†), the bond formation of N1···C6 and N3···C6 at the TSs is confirmed, yielding carbamate anions as the final product. At the TS structures, the difference in the

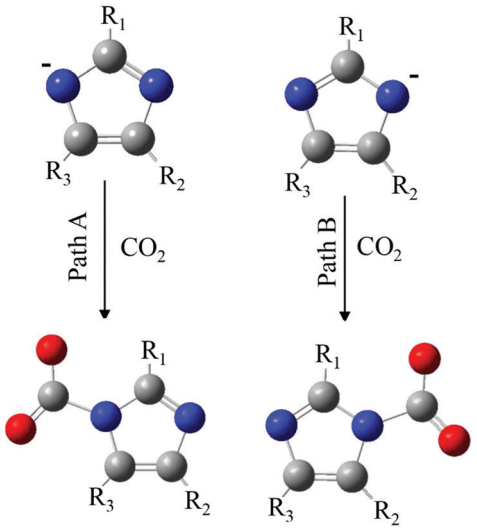

Scheme 2 The proposed mechanism for CO_2 absorption with imidazole anion of DBU-ILs.

bond length of the N1···C6 and N3···C6 interactions, especially in the case of **[DBUH$^+$][2-MeIm$^-$]**, **[DBUH$^+$][2-EtIm$^-$]**, and **[DBUH$^+$][2-Et-4MeIm$^-$]**, indicates that the steric effect of alkyl groups remarkably affects the interaction between CO_2 and the imidazole anion. The CPCM method as an implicit solvent model is not adequate to show the solvent effect on the critical bond at the TSs.

3.2.3 Energy analysis. Theoretical thermodynamic and kinetic parameters during the CO_2 absorption by the DBU-based ILs were calculated and represented in Table 2. The potential energy diagram (PED) for paths A and B in **[DBUH$^+$][Im$^-$]** ILs are represented in Fig. 5 in the gas phase and water (the PED for other DBU-based ILs are represented in Fig. S4, ESI†).

Thermodynamic studies indicate that paths A and B are unfavorable for **[DBUH$^+$][2-PhIm$^-$]** and **[DBUH$^+$][2-Et-4MeIm$^-$]**, respectively ($\Delta G > 0$), while in other ILs, CO_2 is absorbed chemically and the process is exothermic. The lowest $\Delta G^{\neq}$ value is observed in the case of **[DBUH$^+$][Im$^-$]** in the gas phase. The presence of the methyl group at the R_1 and R_2 positions in the cases of **[DBUH$^+$][4-MeIm$^-$]** and **[DBUH$^+$][2-MeIm$^-$]** does not show a significant change in $\Delta G^{\neq}$. On the other hand, on the functionalization of the imidazole anion by ethyl, propyl, and phenyl groups, the energy barrier of the reaction increases, which shows that the steric effect of alkyl groups decreases the interaction ability of the anion with CO_2 molecules. The highest energy barrier is related to **[DBUH$^+$][2-PhIm$^-$]**, in which the electron-withdrawing effect of the phenyl groups decreases the electronic charges on the N1 and N3 atoms that weakens the strength of N3···C6 interaction in comparison with **[DBUH$^+$][Im$^-$]**. In the presence of water, CO_2 absorption by **[DBUH$^+$][Im$^-$]** is more favorable than other DBU-based ILs from the thermodynamics and kinetics points of view. Alkyl groups represent the same behavior in the gas phase.

Overall, the DFT results indicate that **[DBUH$^+$][Im$^-$]** is the preferred candidate for CO_2 absorption in comparison with other ILs, and the alkyl groups on the anion decrease the ability of CO_2 uptake. All DFT results are in agreement with the MD simulations and experiments.[30]

3.2.4 NBO analysis. The stabilization energy, $E(2)$, provides information about the interaction of donor–acceptor orbitals in the reactants and TSs in the CO_2 absorption process. This analysis provides a better insight into the strength of N1···C6 and N3···C6 bond interactions. The stabilization energies of these interactions for different DBU-based ILs are listed in Table S5 (ESI†). On the basis of the obtained results, in all cases, the higher stabilization energies are related to the lone pair electrons of N atoms of the imidazole anions and the antibonding orbital of the C–O bonds. These interactions include lp N1 → π* C6–O8 and lp N3 → π* C6–O8, which confirms the N···C bond formation between the DBU-based ILs and CO_2.

The presence of a methyl group at the R_1 and R_2 positions of **[DBUH$^+$][2-MeIm$^-$]** and **[DBUH$^+$][4-MeIm$^-$]** does not have a

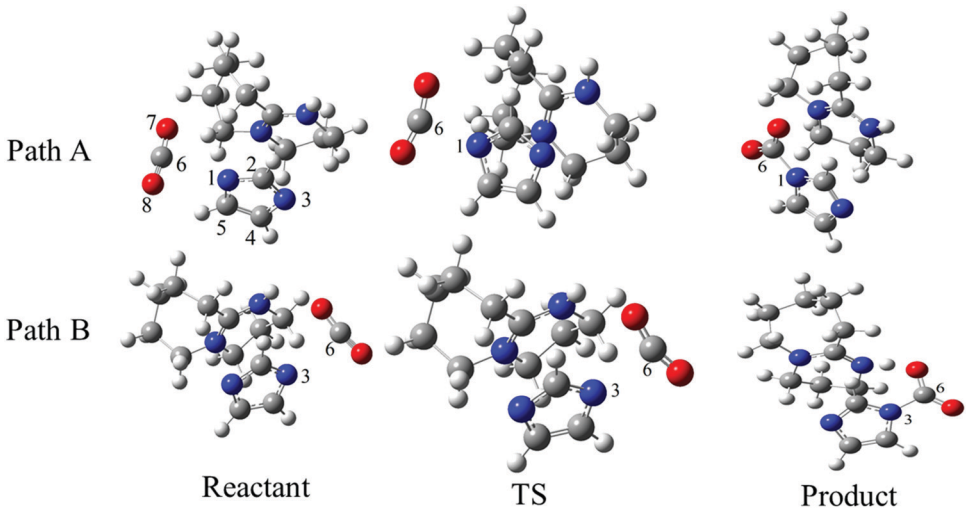

Fig. 4 The optimized structures of the reactants, TSs, and product in **[DBUH$^+$][Im$^-$]** in the proposed paths of the mechanism.

Table 2 Thermodynamic and kinetic parameters of the CO_2 absorption by different DBU-based ILs in the gas phase and water (kJ mol^{-1}, Δs in J mol^{-1} K^{-1})

IL	Path	$\Delta G^{\neq}$	ΔG	ΔH	ΔS	$\Delta G_w^{\neq}$	ΔG_w	ΔH_w	ΔS_w
[DBUH$^+$][Im$^-$]	A	13.50	−38.82	−52.24	−45.04	5.68	−54.63	−64.40	−32.80
	B	7.61	−33.65	−41.34	−25.77	6.87	−52.58	−54.64	−6.92
[DBUH$^+$][4-MeIm$^-$]	A	13.60	−39.99	−51.24	−37.75	7.88	−46.17	−52.48	−21.17
	B	7.13	−36.83	−41.18	−14.58	10.10	−51.32	−55.04	−12.50
[DBUH$^+$][2-MeIm$^-$]	A	14.73	−35.46	−47.48	−40.27	6.63	−46.79	−52.61	−19.85
	B	9.94	−34.79	−43.03	−27.64	7.54	−58.82	−57.85	3.24
[DBUH$^+$][2-EtIm$^-$]	A	21.59	−21.54	−33.31	−39.47	22.65	−39.43	−53.30	−46.51
	B	11.52	−26.16	−40.67	−48.66	23.06	−33.82	−50.88	−57.23
[DBUH$^+$][2-PrIm$^-$]	A	16.38	−40.10	−52.53	−41.66	10.97	−42.31	−47.04	−15.88
	B	9.06	−20.23	−31.67	−38.32	16.05	−37.21	−49.78	−42.17
[DBUH$^+$][2-iPrIm$^-$]	A	16.38	−29.74	−43.53	−46.26	11.89	−31.93	−46.78	−49.80
	B	17.47	−45.35	−54.55	−31.92	20.45	−62.15	−71.96	−32.91
[DBUH$^+$][2-Et-4-MeIm$^-$]	A	19.20	−24.56	−35.76	−37.54	20.43	−42.93	−55.49	−42.11
	B	—	2.54	−15.67	−59.08	26.74	−19.09	−37.44	−61.54
[DBUH$^+$][2-PhIm$^-$]	A	—	28.27	16.77	−38.57	—	11.35	0.814	35.32
	B	37.02	−7.57	−18.04	−35.13	29.56	−16.36	−33.81	−58.54

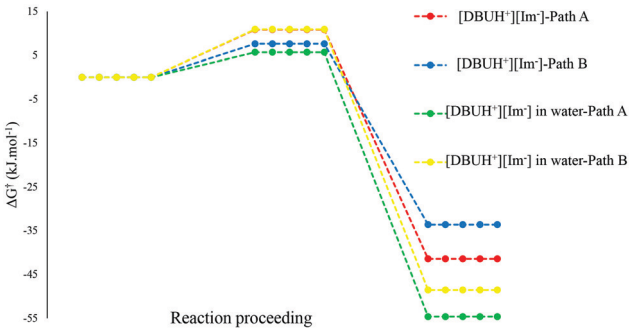

Fig. 5 The potential energy diagram of CO_2 absorption by **[DBUH$^+$][Im$^-$]** in the gas phase and water.

significant effect on lp N1 → π* C6–O8 and lp N3 → π* C6–O8 interactions. The stabilization energy analyses of the **[DBUH$^+$][2-EtIm$^-$]**, **[DBUH$^+$][2-PrIm$^-$]** and **[DBUH$^+$][2-iPrIm$^-$]** ILs indicate that the presence of propyl and iso-propyl groups decreases the donor–acceptor interaction energy at the TS structures that may be related to the steric effects of the alkyl groups. The lowest stabilization energy of lp N3 → π* C6–O7 and lp N3 → π* C6–O8 is found in **[DBUH$^+$][2-PhIm$^-$]**, which indicates the lowest charge transfer in comparison with other ILs, according to the thermodynamic and kinetic results.

3.2.5 QTAIM analysis. To investigate the nature of the anion–CO_2 interactions, topological parameters at the bond critical points (BCPs) of the N1···C6 and N3···C6 for the reactant and TS structures were calculated in the gas phase model by using the QTAIM analysis and represented in Table S6 (ESI†). On the basis of the obtained results, the electron density of N1···C6 and N3···C6 BCP in TSs A and B is more than that of the reactants, which indicates the bond formation between these atoms during the reaction. The theoretical ratio of the kinetic energy density to the potential energy density ($-G/V$) is an indicator of the bond type. The analysis of the $-G/V$ ratio shows that the N···C bond at the TS has a covalence character. To describe the strength of the bond formed at the TSs quantitatively and qualitatively, ELF and LOL parameters were calculated and depicted in Fig. S5 (ESI†). According to this figure, the bond formation between N1···C6 and N3···C6 is confirmed.

4. Conclusion

A joint MD simulation and QM study was performed on the possibility of CO_2 absorption by DBU-based ILs. The anionic parts of these ILs are different in the alkyl groups as the substituent. To show the effect of water molecules as the co-solvent in CO_2 absorption, the implicit solvent model was applied in QM calculations. 20 ns MD simulations in the system consisting of DBU-based ILs and CO_2 molecules indicate that **[DBUH$^+$][Im$^-$]** has the highest ability of CO_2 absorption. On the basis of the obtained results, it was confirmed that ethyl, propyl, iso-propyl, and phenyl substituent groups decrease the strength of the N···C interactions. On the basis of the $N(r)$ values, **[DBUH$^+$][Im$^-$]** is the preferred candidate for CO_2 absorption. Moreover, water molecules decrease the ability of the anion to interact with CO_2, due to the H-bond formation with the N atoms of the imidazole anion, which is in agreement with the experimental data. DFT calculations on the CO_2 absorption show that the presence of ethyl, propyl, iso-propyl, and phenyl groups on the anion increases the activation Gibbs energy of the reaction. This means that the steric and inductive effects of the alkyl groups remarkably affect the thermodynamics and kinetics of the CO_2 uptake. Also, the presence of water molecules has a significant effect on the kinetics of the reaction and increases the energy barrier of the N···C interaction in comparison with the gas phase, especially in the case of alkylated imidazole anions. A good agreement between the MD simulations and QM results with the experimental results indicates that the computational modeling is of interest because it is complementary to the experimental method to design new efficient ILs for industrial processes.

Conflicts of interest

The authors claimed that there is not any conflict of interest.

Acknowledgements

Research Council of the Ferdowsi University of Mashhad is acknowledged for financial support (Grant No. 1/50563). We hereby acknowledge that part of this computation was performed at the Sci-HPC center of the Ferdowsi University of Mashhad.

References

1 S. F. Wang, X. Q. Li, H. Wu, Z. Z. Tian, Q. P. Xin, G. W. He, D. D. Peng, S. L. Chen, Y. Yin, Z. Y. Jiang and M. D. Guiver, *Energy Environ. Sci.*, 2016, **9**, 1863.
2 R. Ben-Mansour, M. A. Habib, O. E. Bamidele, M. Basha, N. A. A. Qasem, A. Peedikakkal, T. Laoui and M. Ali, *Appl. Energy*, 2016, **161**, 225.
3 G. George, N. Bhoria, S. AlHallaq, A. Abdala and V. Mittal, *Sep. Purif. Technol.*, 2016, **158**, 333.
4 K. Huang, X. M. Zhang, X. B. Hu and Y. T. Wu, *AIChE J.*, 2016, **62**, 4480.
5 K. Huang, X. M. Zhang, Y. Xu, Y. T. Wu, X. B. Hu and Y. Xu, *AIChE J.*, 2014, **60**, 4232.
6 K. Huang, D. N. Cai, Y. L. Chen, Y. T. Wu, X. B. Hu and Z. B. Zhang, *ChemPlusChem*, 2014, **79**, 241.
7 X. Y. Liu, Y. Huang, Y. S. Zhao, R. Gani, X. P. Zhang and S. J. Zhang, *Ind. Eng. Chem. Res.*, 2016, **55**, 5931.
8 Y. Huang, X. P. Zhang, X. Zhang, H. F. Dong and S. J. Zhang, *Ind. Eng. Chem. Res.*, 2014, **53**, 11805.
9 P. A. Hunt, *J. Phys. Chem. B*, 2007, **111**, 4844.
10 M. Kohagen, M. Brehm, Y. Lingscheid, R. Giernoth, J. Sangoro, F. Kremer, S. Naumov, C. Iacob, J. Kärger, R. Valiullin and B. Kirchner, *J. Phys. Chem. B*, 2011, **115**, 15280.
11 T. Welton, *Chem. Rev.*, 1999, **99**, 2071.
12 S. Singh, I. Bahaduv, P. Naidoo, G. Redhi and D. Ramjugernath, *J. Mol. Liq.*, 2016, **220**, 33.
13 F. van Rantwijk and R. A. Sheldon, *Chem. Rev.*, 2007, **107**, 2757.
14 R. A. Sheldon, R. M. Lau, M. J. Sorgedrager, F. van Rantwijk and K. R. Seddon, *Green Chem.*, 2002, **4**, 147.
15 N. V. Plechkova and K. R. Seddon, *Chem. Soc. Rev.*, 2008, **37**, 123.
16 M. J. Earle and K. R. Seddon, *Pure Appl. Chem.*, 2000, **72**, 1391.
17 A. L. Revelli, F. Mutelet and J. N. Jaubert, *J. Phys. Chem. B*, 2010, **114**, 12908.
18 M. Rezaeian, M. Izadyar and A. Nakhaeipour, *J. Phys. Chem. A*, 2018, **122**(26), 5721.
19 Z. Z. Yang, Y. N. Zhao and L. N. He, *RSC Adv.*, 2011, **1**, 545.
20 H. Oediger, F. Moller and K. Eiter, *Synthesis*, 1972, 591.
21 R. Reed, R. Réau, F. Dahan and G. Bertrand, *Angew. Chem., Int. Ed. Engl.*, 1993, **32**, 399.
22 S. N. Shah, M. Ismail, M. I. A. Mutalib, R. B. M. Pilus and L. K. Chellappan, *Fuel*, 2016, **181**, 579.
23 F. Liu, J. Guo, P. Zhao, Y. Gu, J. Gao and M. Liu, *Polym. Degrad. Stab.*, 2019, **167**, 124.
24 Y. Zhao, J. Qiu, L. Tian, Zh. Li, M. Fan and J. Wang, *ACS Sustainable Chem. Eng.*, 2016, **4**, 5553.
25 Ch. Yang, M. Liu, J. Zhang, X. Wang, Y. Jiang and J. Sun, *Mol. Catal.*, 2018, **450**, 39.
26 E. Privalova, M. Nurmi, M. S. Maranon, E. V. Murzina, P. Maki-Arvela, K. Eranen, D. Yu Murzin and J. P. Mikkola, *Sep. Purif. Technol.*, 2013, **107**, 340.
27 K. C. Lethesh, S. N. Shah and M. I. A. Mutalib, *J. Chem. Eng. Data*, 2014, **59**, 1788.
28 K. Chen, G. Shi, W. Zhang, H. Li and C. Wang, *J. Am. Chem. Soc.*, 2016, **138**, 14198.
29 T. Kddermann, C. Wertz, A. Heintz and R. Ludwig, *Angew. Chem., Int. Ed.*, 2006, **45**, 3697.
30 X. Zhu, M. Song and Y. Xu, *ACS Sustainable Chem. Eng.*, 2017, **5**, 8192.
31 A. G. Ying, L. Liu, G. F. Wu, X. Z. Chen, W. D. Ye, J. H. Chen and K. Y. Zhang, *Chem. Res. Chin. Univ.*, 2009, **25**, 876.
32 J. Hu, J. Ma, Q. Zhu, Zh. Zhang, C. Wu and B. Han, *Angew. Chem., Int. Ed.*, 2015, **54**, 1.
33 W. Li, W. Cheng, X. Yang, Q. Su, L. Dong, P. Zhang, Y. Yi, B. Li and S. Zhang, *Chin. J. Chem.*, 2018, **36**, 293.
34 B. Wang, Zh. Luo, E. H. M. Elageed, Sh. Wu, Y. Zhang, X. Wu, F. Xia, G. Zhang and G. Gao, *ChemCatChem*, 2016, **8**, 830.
35 X. Zhang, X. Liu, X. Yao and S. Zhang, *Ind. Eng. Chem. Res.*, 2011, **50**, 8323.
36 D. A. Case, T. A. Darden, T. E. Cheatham, C. L. Simmerling, J. Wang, R. E. Duke, R. Luo, R. C. Walker, W. Zhang, K. M. Merz, B. Roberts, S. Hayik, A. Roitberg, G. Seabra, J. Swails, A. W. Götz, I. Kolossváry, K. F. Wong, F. Paesani, J. Vanicek, R. M. Wolf, J. Liu, X. Wu, S. R. Brozell, T. Steinbrecher, H. Gohlke, Q. Cai, X. Ye, J. Wang, J. Hsieh, G. Cui, D. R. Roe, D. H. Mathews, M. G. Seetin, R. Salomon-Ferrer, C. Sagui, V. Babin, T. Luchko, S. Gusarov, A. Kovalenko and P. A. Kollman, *AMBER 12*, University of California, San Francisco, 2012.
37 H. Heinz, R. Vaia, B. Farmer and R. Naik, *J. Phys. Chem. C*, 2008, **112**, 17281.
38 J. Wang, R. M. Wolf, J. W. Caldwell, P. A. Kollamn and D. A. Case, *J. Comput. Chem.*, 2004, **25**, 1157.
39 L. Martinez, R. Andrade, E. G. Birgin and J. M. Martinez, *J. Comput. Chem.*, 2009, **30**, 2157.
40 B. P. Uberuaga, M. Anghel and A. F. Voter, *J. Chem. Phys.*, 2004, **120**, 6363.
41 D. J. Sindhikara, S. Kim, A. F. Voter and A. E. Roitberg, *J. Chem. Theory Comput.*, 2009, **5**, 1624.
42 J. P. Ryckaert, G. Ciccotti and H. J. C. Berendsen, *J. Comput. Phys.*, 1977, **23**, 327.
43 U. Essman, L. Perera, M. Berkowitz, T. Darden, H. Lee and L. Pedersen, *J. Chem. Phys.*, 1995, **103**, 8577.
44 M. J. Frisch, G. W. Trucks, H. B. Schlegel, G. E. Scuseria, M. A. Robb, J. R. Cheeseman, J. A. Montgomery, T. Vreven, K. N. Kudin and J. C. Burant, *et al.*, *Gaussian 09*, Gaussian, Inc., Pittsburgh, PA, 2009.
45 Y. Zhao and D. G. Truhlar, *Functionals Theor. Chem. Acc.*, 2008, **120**, 215.
46 J. Kona and W. M. F. J. Fabian, *J. Chem. Theory Comput.*, 2011, **7**, 2610.

47 H. B. Schlegel, C. Peng, P. Y. Ayala and M. J. Frisch, *J. Comput. Chem.*, 1996, **17**, 49.
48 M. Cossi, N. Rega, G. Scalmani and V. Barone, *J. Comput. Chem.*, 2003, **24**, 669.
49 M. Cossi, V. Barone, R. Cammi and J. Tomasi, *Chem. Phys. Lett.*, 1996, **255**, 327.
50 A. E. Reed, L. A. Curtiss and F. Weinhold, *Chem. Rev.*, 1988, **88**, 899.
51 R. F. W. Bader, *Atoms in Molecules, A Quantum Theory*, Oxford University Press, New York, 1990.
52 T. Lu and W. Chen, *J. Comput. Chem.*, 2012, **33**, 580.
53 G. A. Jeffrey, *An Introduction to Hydrogen Bonding*, Oxford University Press, 1997.
54 X. Lei, Y. Xu, L. Zhu and X. Wang, *RSC Adv.*, 2014, **4**, 7052.
55 M. Pan, N. Cao, W. Lin, X. Luo, K. Chen, S. Che, H. Li and C. Wang, *ChemSusChem*, 2016, **9**, 2351.